

Effect of Ce-modified Fe/ZSM-5 zeolite for selective catalytic reduction of NO_x by ammonia

Li Chenxi¹, Meng Fanwei¹ and Ye Qing^{1,a}

¹Key Laboratory of Beijing on Regional Air Pollution Control, Department of Environmental Science, College of Environmental and Energy Engineering, Beijing University of Technology, Beijing 100124, China

Abstract. A series of *x*Ce-Fe/ZSM-5 (*x* = 0, 0.25, 0.5 wt%) samples were prepared by the impregnation method, and the catalytic activity was evaluated by the selective catalytic reduction of NO_x with ammonia (NH₃-SCR). The physicochemical properties of prepared samples were characterized by various techniques such as X-ray diffraction (XRD), Brunner-Emmet-Teller (BET) measurement, hydrogen temperature-programmed reduction (H₂-TPR), X-ray photoelectron spectroscopy (XPS), ammonia temperature-programmed desorption (NH₃-TPD) and in situ diffuse reflectance infrared Fourier transform spectroscopy (in situ DRIFTS). XRD and BET results demonstrated that Ce and Fe species were uniform dispersed on the surface of the ZSM-5 zeolite and the micropore structure of ZSM-5 was still maintained. H₂-TPR analysis indicated that the doping of Ce created more isolated Ce⁴⁺ and Fe³⁺ on the surface of catalysts, and the abundant Ce⁴⁺ and Fe³⁺ could enhance the reduction ability of catalysts. XPS analysis suggested that the doping of Ce could generate more oxygen vacancies, thereby increasing the number of chemisorption oxygen. According to the in-situ DRIFTS and NH₃-TPD results, Ce species provided more acidic sites, which is beneficial to the NH₃ adsorption ability of ZSM-5 zeolite. Additionally, the abundant chemisorption oxygen, medium and strong Brønsted acid sites, excellent NH₃ adsorption ability and outstanding reduction property are beneficial to the NH₃-SCR reaction. Among all prepared samples, the 0.25Ce-Fe/ZSM-5 sample possessed the widest reaction temperature window and the best catalytic performance (NO conversion over 98% at 350–450 °C), which was associated with the abundant acid sites and remarkable adsorption ability of NH₃, outstanding redox ability and abundant chemisorption oxygen after the doping of Ce.

1 Introduction

Nitrogen oxides (NO_x) emitted from vehicle exhaust have been a major source of atmospheric pollution which are considered as one of the main contributors to environmental destruction, such as photochemical smog, acid rain, ozone depletion and the greenhouse effect. Due to the masses of environmental problems and serious damage to human health resulted by NO_x, the emission limit regulations for vehicles have been made more stringent throughout the world^[1]. Selective catalytic reduction of nitrogen oxides with NH₃ (NH₃-SCR) is a well-developed technology that has been extensively studied. Recently, vanadium catalysts (V₂O₅/TiO₂/WO₃) showed remarkable catalytic activity in SCR reaction that have been commercialized. Although commercial vanadium catalysts exhibited excellent activity, it still remains some problems, such as the toxicity of vanadium, narrow activity window and serious oxidation of ammonia at high temperatures^[2]. Thus, it is extremely urgent to develop environmentally friendly NH₃-SCR catalysts with a wide activity window and high nitrogen selectivity. Nowadays, zeolite-based catalysts such as ZSM-5, BETA, SSZ, SAPO and BEA have been attracted

extensive attention. Among them, the most extensive research has focused on the metal ion-exchanged ZSM-5 zeolite demonstrates due to the excellent SCR catalytic activity caused by its unique three-dimensional pore structure, large specific surface area, abundant acid sites and superior stability, which have been widely applied in NH₃-SCR system. It has been reported that Fe-exchanged zeolite catalysts exhibited outstanding catalytic activity and superior stability and N₂ selectivity in NH₃-SCR reaction. BOUBNOV et al.^[3] indicated that Fe active component of Fe-zeolite catalysts not only possessed the ability to coordinate NO_x but also adsorbed ammonia and water. IWASAKI et al.^[4] studied the effect of various preparation methods for SCR activity over Fe/ZSM-5, demonstrated that the SCR activity was more related to the preparation method than the Fe doping content.

Although Fe/ZSM-5 catalyst showed outstanding catalytic activity in high-temperature range, limited catalytic performance is obtained in a lower temperature range. Thus, the addition of extra-metal ions to further promote the catalytic performance of Fe/ZSM-5 catalyst in lower temperatures could be feasible. Ce is a common rare earth metal which possessed strong oxygen storage ability and excellent oxidation performance. In the

^a Ye Qing: yeqing@bjut.edu.cn

previous work, we determined the optimal catalyst preparation conditions and the amount of Fe doping (1.4 wt%). The purpose of this work is to determine the optimal Ce/Fe ratio and explore the relationship between the physicochemical properties and SCR activity of the catalysts.

2 EXPERIMENTAL

2.1 Catalyst preparation

The ZSM-5 zeolites (Si/Al = 50) were obtained from the Dalian Institute of Chemical Physics, China. Fe/ZSM-5 and Ce/ZSM-5 samples were prepared by separately impregnating the ZSM-5 zeolite with 1.4 wt% $\text{FeCl}_2 \cdot 4\text{H}_2\text{O}$ and 0.25 wt% $\text{CeN}_3\text{O}_9 \cdot 6\text{H}_2\text{O}$. And then the obtained suspension was stirred for 1 h at 60 °C, after stirring the suspension was evaporated using a rotary vacuum evaporator. After that, the obtained powders were calcined in muffle furnace at 500 °C for 5 h, with a product denoted as Fe/ZSM-5 and Ce/ZSM-5 catalysts, respectively. $x\text{Ce-Fe/ZSM-5}$ samples ($x=0.25, 0.5$ wt%) were prepared by the Fe/ZSM-5 sample impregnating with the $\text{CeN}_3\text{O}_9 \cdot 6\text{H}_2\text{O}$ aqueous solution, and the following process is similar to the above.

2.2 Catalyst characterization

The crystal phases of the samples were analyzed by XRD, and the patterns of samples were analyzed on a Bruker D8 advance diffractometer with Cu $K\alpha$ radiation. Specific surface areas were calculated based on the BET method. The pore size distributions were calculated by applying the Barrett-Joyner-Halenda (BJH) method. XPS were used to determine surface compositions and oxidation states of the metal on the surface of the samples. H_2 -TPR experiments were performed on a Builder (PCA-1200), and NH_3 -TPD experiments were performed using a Builder PCA-1200 analyzer. In-situ DRIFTS experiments were conducted on a Bruker spectrometer equipped with a high reaction chamber.

2.3 NH₃-SCR activity evaluation

The SCR activity of the catalyst samples was evaluated at atmospheric pressure in a fixed-bed continuous flow quartz reactor. About 300 mg of catalyst samples (60-80 mesh) were utilized in experiments. The reactant gases were mixtures of 500 ppm NO, 500 ppm NH_3 , 10% O_2 , 10% H_2O , with N_2 as the balance. The total gas flow rate was 300 mL/min, and the gas hourly space velocity was 33,000 h^{-1} . The concentration of NO in the effluent gas stream was measured using a Thermo Model 42 i-HL. NO conversion is defined as follows:

$$X_{\text{NO}} = \frac{[\text{NO}]_{\text{inlet}} - [\text{NO}]_{\text{outlet}}}{[\text{NO}]_{\text{inlet}}} \times 100(\%) \quad (1)$$

where $[\text{NO}]_{\text{inlet}}$ and $[\text{NO}]_{\text{outlet}}$ represent the concentrations of NO in the inlet and outlet gas streams, respectively.

3 RESULTS AND DISCUSSION

3.1. NH₃-SCR activity

The NO conversion of the prepared zeolite samples was evaluated using the SCR of NO_x with NH₃, and the results are shown in Fig 1. As shown in Fig 1, NO conversion over each of the samples possessed an obvious increase with the increase of temperature from 150 °C to 450 °C, but decreased slightly from 450 °C to 550 °C.

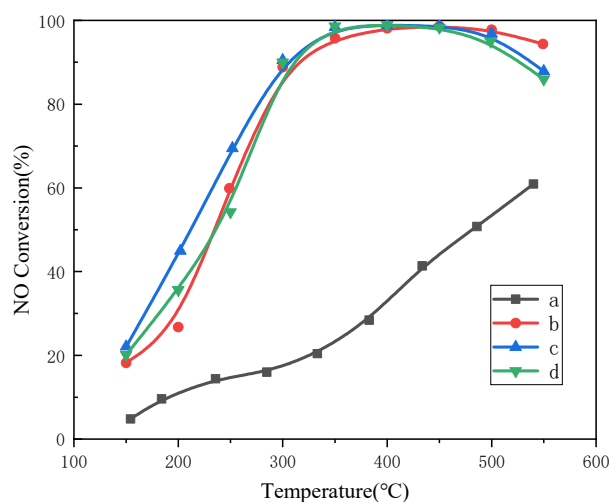


Figure 1. The NO conversion of the various ZSM-5 catalysts. (a: Ce/ZSM-5, b: Fe/ZSM-5, c:0.25Ce-Fe/ZSM-5, d: 0.5Ce-Fe/ZSM-5.)

According to our previous studies^[5], the optimal doped content of Fe for Fe/ZSM-5 was 1.4 wt% which exhibited the best activity for SCR. As can be seen, the Fe/ZSM-5 sample exhibited a NO conversion over 90% at 300-550 °C, whereas the activity was unsatisfactory in lower-temperature in 150-300 °C ranges. After Ce doping, 0.25Ce-Fe/ZSM-5 sample showed a higher NO conversion than Fe/ZSM-5 in the temperatures range from 150-450 °C. It is obvious that the catalytic activity of Fe/ZSM-5 sample promoted after Ce species doping, indicating that Ce introduction exhibit a significant enhancement of catalytic activity. Furthermore, the catalytic activity of the 0.5Ce-Fe/ZSM-5 sample decreased slightly with the increase of Ce doping. Compared with 0.25Ce-Fe/ZSM-5 sample, 0.5Ce-Fe/ZSM-5 sample showed the lower NO conversion in the whole reaction. Among the all evaluated samples, 0.25Ce-Fe/ZSM-5 sample showed the best catalytic activity and the widest reaction window (over than 98% NO conversions in the temperature range of 350-450 °C), indicating that the optimal doping content of Ce species is 0.25 wt% and there existed an interaction between Fe and Ce, which might be a crucial factor in promoting higher NO conversion at low temperatures. To investigate the effect of single Ce-doped Ce/ZSM-5 sample was prepared. As shown in Fig 1, the 0.25Ce/ZSM-5 sample showed a poor catalytic activity, only achieved 63% NO conversion at 550 °C, indicating that Ce does not act as an active species.

3.2 XRD and BET analysis

XRD analysis was performed to investigate the crystal structures of the catalyst samples (not shown). The diffraction peaks at 2θ of 7.9° , 8.8° , 23.1° , and 23.8° were detected in all samples, which are attributed to characteristic diffraction signals of the ZSM-5 zeolite^[6], illustrating that the catalysts maintained the original crystal structure of the ZSM-5 zeolite.

Specific surface area and pore volumes of all samples in order of decreasing sequence are Fe/ZSM-5 ($445.99 \text{ m}^2/\text{g}$, $0.177 \text{ cm}^3/\text{g}$) > Ce/ZSM-5 ($399.09 \text{ m}^2/\text{g}$, $0.161 \text{ cm}^3/\text{g}$) > 0.25Ce-Fe/ZSM-5 ($384.41 \text{ m}^2/\text{g}$, $0.155 \text{ cm}^3/\text{g}$) > 0.5Ce-Fe/ZSM-5 ($379.68 \text{ m}^2/\text{g}$, $0.153 \text{ cm}^3/\text{g}$). The results demonstrate that the specific surface area, average pore size and total pore volume of the Fe/ZSM-5 sample surpass those of the Ce/ZSM-5 and xCe-Fe/ZSM-5 ($x = 0.25, 0.5 \text{ wt}\%$) samples. These results suggest that the surface areas, pore volume and the N_2 adsorption sites on the surface of the ZSM-5 zeolites were covered by Ce species. Compared with the results of the catalytic activity, the order of the specific surface area of the samples was inconsistent with the SCR activity of the samples, indicating that the specific surface area of the samples was not the crucial factor.

3.3 H_2 -TPR analysis

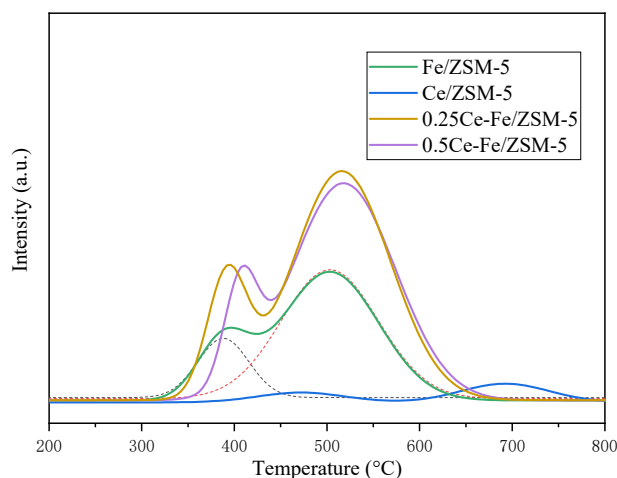


Figure 2. H_2 -TPR profiles of catalysts.

To investigate the reduction ability of active species on the samples, H_2 -TPR analysis was performed, and the results are illustrated in Fig 2. As shown in Fig 2, each sample showed two reduction peaks. For Fe/ZSM-5 (a) sample, a weak reduction peak appeared at around 400°C and a strong peak at around 500°C . The former weak peak was attributed to the reduction of $\text{Fe(III)} \rightarrow \text{Fe(II)}$, including the reduction of isolated Fe^{3+} species and oligomeric Fe_2O_3 species^[7]. The second peak was attributed to the reduction of $\text{Fe(II)} \rightarrow \text{Fe(0)}$, including the reduction of Fe_3O_4 and FeO ^[8]. It has been reported that the reduction of high-polymer Fe oxide particles appears at over 730°C , but no reduction peak attribute to Fe species was observed over 700°C for the samples, indicating that high-polymer Fe oxide particles were absent in the Fe/ZSM-5 sample, and these results were

consistent with the XRD results. Ce/ZSM-5 sample exhibited a weak reduction peak appear at 465°C which ascribed to the reduction of $\text{Ce}^{4+} \rightarrow \text{Ce}^{3+}$, while the slightly stronger peak at 700°C was ascribed to the reduction of CeO_2 ^[9]. The total hydrogen consumption of Ce/ZSM-5 catalyst was $0.021 \text{ mmol}/\text{g}^{-1}$. For 0.25Ce-Fe/ZSM-5 and 0.5Ce-Fe/ZSM-5 samples, reduction peaks appeared around at 400°C and 515°C . According to the reduction results of single-loaded Fe and single-loaded Ce samples, the peak at 400°C was attributed to the reduction of $\text{Fe}^{3+} \rightarrow \text{Fe}^{2+}$ and $\text{Ce}^{4+} \rightarrow \text{Ce}^{3+}$, whereas the peak at 510°C was explained by the reduction of $\text{Fe}^{2+} \rightarrow \text{Fe}^0$ and CeO_2 .

After quantitative analysis, the hydrogen consumption and peak positions are summarized as follows. The hydrogen consumption decreased in the order of 0.25Ce-Fe/ZSM-5 ($0.294 \text{ mmol}\cdot\text{g}^{-1}$) > 0.5Ce-Fe/ZSM-5 ($0.287 \text{ mmol}\cdot\text{g}^{-1}$) > Fe/ZSM-5 ($0.185 \text{ mmol}\cdot\text{g}^{-1}$) > Ce/ZSM-5 ($0.041 \text{ mmol}\cdot\text{g}^{-1}$). It can be seen that the hydrogen consumption of Ce/ZSM-5 sample was extremely lower than other samples, indicating that the reduction property of Ce species was not significant. For Fe/ZSM-5 sample, the hydrogen consumption was below those for the 0.25Ce-Fe/ZSM-5 and 0.5Ce-Fe/ZSM-5 samples, suggesting that there was a strong interaction between Ce and Fe species, and the strong interaction led to the increase of hydrogen consumption. Compared with 0.5Ce-Fe/ZSM-5 sample, 0.25Ce-Fe/ZSM-5 sample exhibited higher hydrogen consumption, and the first reduction peak of 0.25Ce-Fe/ZSM-5 sample shifted to a lower temperature. This result proved that the reducibility of 0.25Ce-Fe/ZSM-5 sample was better than 0.5Ce-Fe/ZSM-5 sample.

Consequently, 0.25Ce-Fe/ZSM-5 exhibited the most effective reduction peak area and lower reduction peak temperature. Thus, 0.25Ce-Fe/ZSM-5 sample achieved the best NH_3 -SCR activity, which is consistent with the order of catalytic activity in SCR reaction.

3.4 XPS analysis

XPS analysis is used to investigate the surface compositions and chemical states on the surface of prepared samples are shown in Fig 3. Fig 3 presented the Fe 2p and Ce 3d XPS spectra of the various samples. For the Fe 2p spectra, the banding energy around at 707 eV and 725 eV were ascribed to the Fe^{2+} species, whereas the banding energy around at 730 eV and 710 eV were assigned to the Fe^{3+} species, indicating that both Fe^{2+} and Fe^{3+} exist on the catalysts^[10]. The proportions of $\text{Fe}^{2+}/\text{Fe}^{3+}$ were calculated from the relative areas of the corresponding peaks, and the $\text{Fe}^{2+}/\text{Fe}^{3+}$ ratio of the samples decreased in the order of 0.25Ce-Fe/ZSM-5 (0.84) > 0.5Ce-Fe/ZSM-5 (0.76) > Fe/ZSM-5 (0.56). The valence changes of these two elements increased the number of oxygen vacancies, which results in an increase in the lattice oxygen content that in turn promoted the redox process. According to the literatures^[11], Fe^{3+} sites may facilitate the reduction of NO at low temperature. Thus, it could also be one of the reasons why 0.25Ce-Fe/ZSM-5 sample exhibited better NH_3 -SCR performance.

The Ce 3d XPS spectra reveals that two valence states Ce ions for all Ce doping samples and the banding energy around at 887 eV and 905 eV are ascribed to the Ce³⁺ species, whereas the banding energy around at 884 eV, 893 eV, 898 eV, 907 eV and 915 eV were assigned to the surface Ce⁴⁺ species^[12]. The concentrations of Ce⁴⁺ and Ce³⁺ species on the sample surface were calculated from the relative areas of the corresponding peaks, and the Ce³⁺/Ce⁴⁺ ratio of the samples decreased in the order of 0.25Ce-Fe/ZSM-5 (0.48) > 0.5Ce-Fe/ZSM-5 (0.46) > Ce/ZSM-5 (0.44).

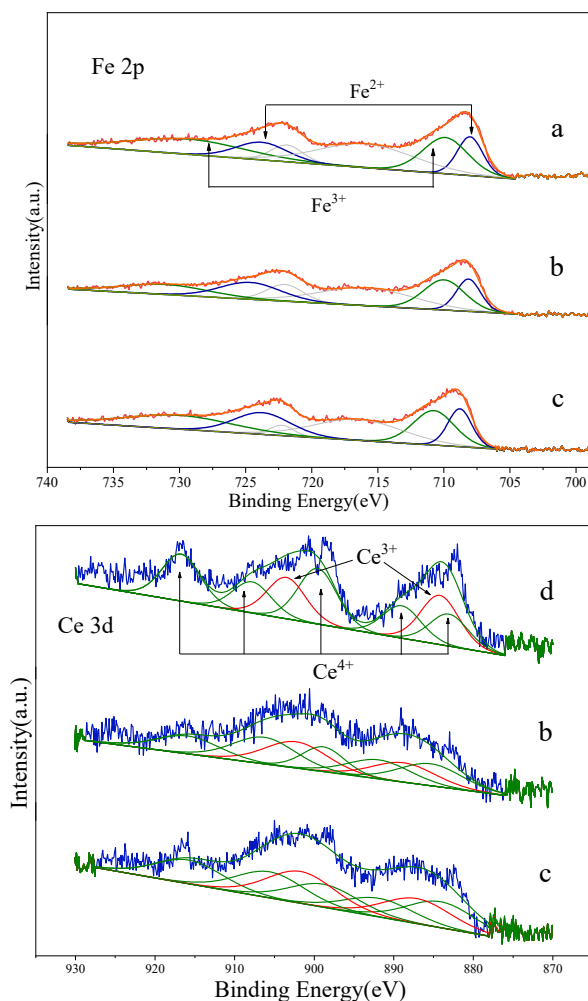


Figure 3. XPS spectra of (a) Fe/ZSM-5, (b) 0.25Ce-Fe/ZSM-5, and (c) 0.5Ce-Fe/ZSM-5, and (d) Ce/ZSM-5

It is clear that there was co-existence of Ce³⁺ and Ce⁴⁺ species on the surface of the samples, indicating that the catalyst surface was not completely oxidized. It is beneficial to the creation of charge imbalance to further form oxygen vacancies, since the electron trapping effect of oxygen vacancies could reduce Ce⁴⁺ to Ce³⁺, and the Ce³⁺ species could produce oxygen vacancies and unsaturated chemical bonds on the sample surface which is responsible for an increase in the amount of the chemisorbed oxygen species^[13].

Compared with other samples, the 0.25Ce-Fe/ZSM-5 sample possessed more Ce³⁺ species and hence more active adsorbed oxygen species on the sample surface, resulting in the best catalytic activity. Meanwhile, abundant Ce³⁺ species could be enhanced the reduction

performance of the samples, which was consistent with the results of H₂-TPR.

3.5 Acidity

The adsorption and activation ability of NH₃ species on the surface of the catalysts is an important factor for the NH₃-SCR reaction. Therefore, the adsorption of NH₃ on the catalyst of each sample was investigated by NH₃-TPD analysis and the result profiles are shown in Fig 4. It can be observed that each sample exhibited three desorption peaks. In general, the NH₃ desorption peak appeared at 230 °C assigned to weak Lewis acid sites with NH₃ adsorbing on the weak Lewis acid sites of surface hydroxyl groups. The second peak appeared at around 350 °C is attributed to medium acidity and mainly related to Lewis acid in the zeolite skeleton and a part of the Lewis acid sites produced by Fe²⁺, Fe³⁺, and Ce³⁺, whereas the high-temperature desorption peak appeared at approximately 450 °C was assigned to the strong acidity from the NH₃ adsorbed on Brønsted acid sites in the zeolite^[14].

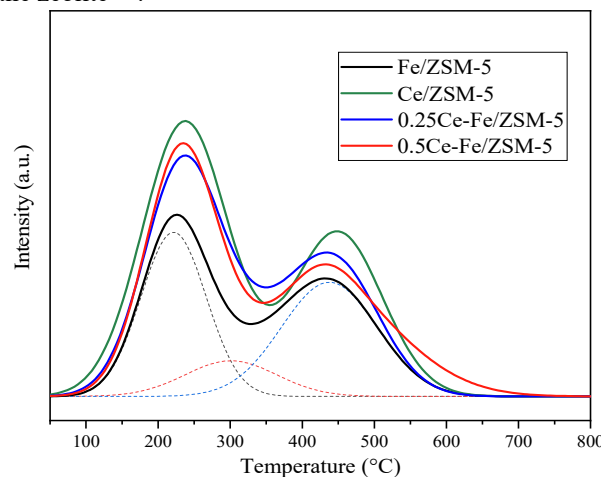


Figure 4. NH₃-TPD profiles of ZSM-5 catalysts.

After curve-fitting of the NH₃-TPD profiles, the desorption peaks and amount of acid sites of each sample are calculated. The total NH₃ desorbed decreased in the order of Ce/ZSM-5 (0.80 mmol/g⁻¹) > 0.5Ce-Fe/ZSM-5 (0.74 mmol/g⁻¹) > 0.25Ce-Fe/ZSM-5 (0.73 mmol/g⁻¹) > Fe/ZSM-5 (0.58 mmol/g⁻¹). The medium acidity of samples decreased in the order of 0.25Ce-Fe/ZSM-5 (0.14 mmol/g⁻¹) > Ce/ZSM-5 (0.13 mmol/g⁻¹) > 0.5Ce-Fe/ZSM-5 (0.06 mmol/g⁻¹) > Fe/ZSM-5 (0.05 mmol/g⁻¹).

It is observed that the total acidity and medium acidity of the Fe/ZSM-5 sample were below those for the 0.25Ce-Fe/ZSM-5 and 0.5Ce-Fe/ZSM-5 samples. The result demonstrates that the interaction between the Ce³⁺ and Brønsted sites on the ZSM-5 zeolite increased the amount of medium and strong acid sites. Thus, Ce/ZSM-5 sample exhibited the most abundant total acid sites, indicating that the loading of Ce enhances the acid sites of the zeolite. As can be seen the 0.25Ce-Fe/ZSM-5 sample showed abundant medium acidity sites (0.137 mmol/g⁻¹). Although 0.5Ce-Fe/ZSM-5 sample doped more Ce than 0.25Ce-Fe/ZSM-5 sample, 0.5Ce-Fe/ZSM-5 sample possessed a lower amount of medium acidity

($0.055 \text{ mmol/g}^{-1}$), which caused by the excessive Ce oxides block on the acidity sites of the ZSM-5 zeolite. As is known to all, medium acidity is a crucial factor in the NH_3 -SCR reaction^[15], the higher medium acidity maintained, the better the activity of the catalyst achieved. Moreover, 0.25Ce-Fe/ZSM-5 sample owned abundant medium acid sites and total acid sites, which is beneficial to the NH_3 -SCR reaction. Compared with the evaluation of NO conversion, indicating that the medium acidity significantly influenced the catalytic activity of the NH_3 -SCR at high temperature. Therefore, 0.25Ce-Fe/ZSM-5 sample exhibited excellent catalytic performance in the wide temperature range which was consistent with the order of catalytic activity.

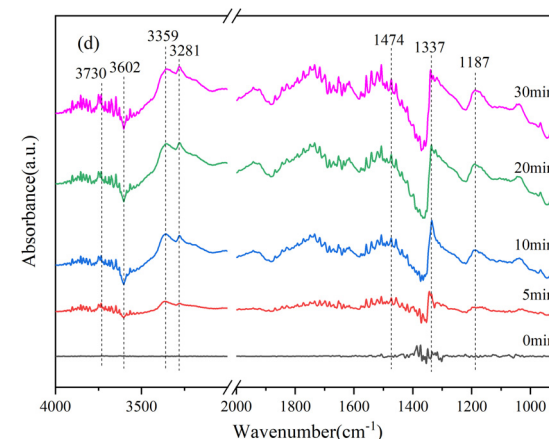
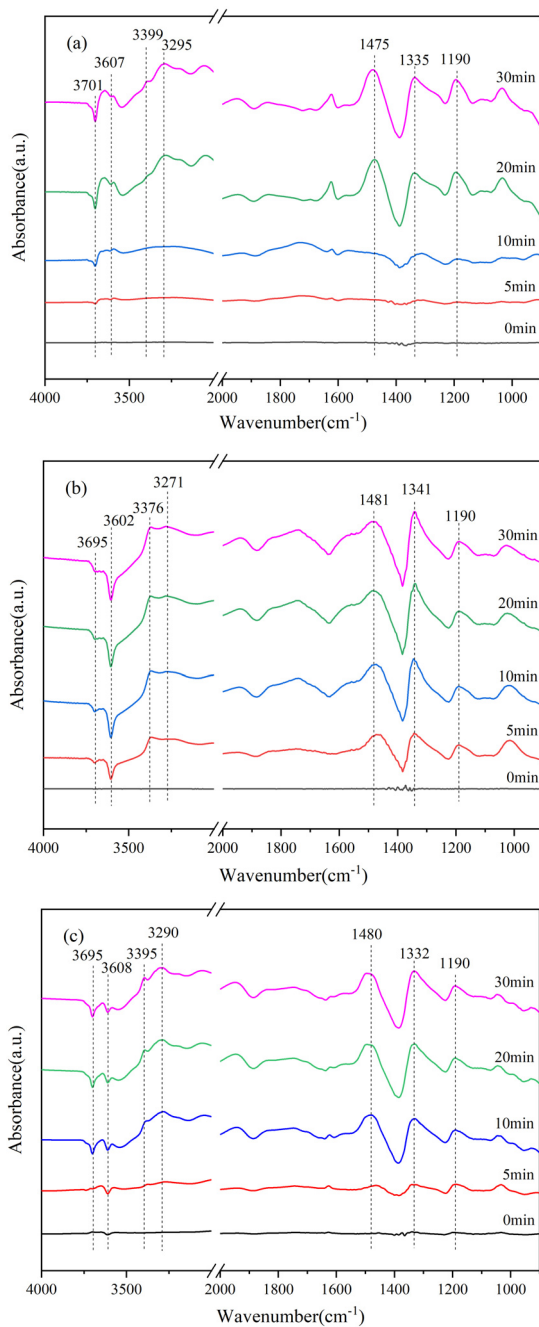


Figure 5. In-situ DRIFTS spectra of NH_3 adsorption. (a) Fe/ZSM-5, (b) Ce/ZSM-5, (c) 0.25Ce-Fe/ZSM-5 , (d) 0.5Ce-Fe/ZSM-5

In situ DRIFT experiments are used to investigate the adsorption phenomenon of reactant molecules on the catalyst surface, which has been considered to play a crucial role in the NH_3 -SCR reaction. To further investigate the NH_3 adsorption performance of ZSM-5 samples, the sample was exposed in a flow of 500 ppm NH_3 at 30°C for 30 min and then purged by N_2 for 30 min. The DRIFTS spectra of the NH_3 adsorption for the various samples are shown in Fig 5, respectively. After the NH_3 adsorption, the samples were covered by NH_3 species. A strong band appeared around at 1335 cm^{-1} and 1475 cm^{-1} while weak bands around at 1190 cm^{-1} , 3300 cm^{-1} , 3400 cm^{-1} , 3600 cm^{-1} and 3700 cm^{-1} . The band appeared at 1475 cm^{-1} could be caused by NH_4^+ species on Brønsted acid sites and the band appeared at 1335 cm^{-1} could be attributed to the interaction between NH_3 and surface oxygen^[16].

The bands appeared at 3700 cm^{-1} and 3600 cm^{-1} were ascribed to the O-H stretching vibration modes which were caused by strong interactions between the surface hydroxyls and the NH_3 . The bands that appeared at $3400\text{--}3000 \text{ cm}^{-1}$ were assigned to the stretching vibrations of N-H bonds, whereas the bands at 1190 cm^{-1} were attributed to coordinated NH_3 on Lewis acid sites^[17]. With time increasing, the intensity of the band appeared at 1475 cm^{-1} , 1335 cm^{-1} and 1190 cm^{-1} increased, indicating that increasing NH_3 species were adsorbed on the surface of the each of samples. For Fe/ZSM-5 sample, the bands assigned to Lewis acid sites and Brønsted acid sites were increased slower than Ce/ZSM-5 and $x\text{Ce-Fe/ZSM-5}$ sample, indicating that Ce/ZSM-5 and $x\text{Ce-Fe/ZSM-5}$ sample reached adsorption saturation more quickly. Above all results demonstrate that doping of Ce on the Fe/ZSM-5 catalysts effectively enhances its Lewis acid and Brønsted acidity, and the manifestation was the band appeared at 1475 cm^{-1} , 1332 cm^{-1} and 1190 cm^{-1} increased. This result illustrates that the doping of Ce could enhance the amount of acid sites on the ZSM-5 zeolite and promoted the adsorption ability of NH_3 , which was also consistent with the results of the NH_3 -TPD analysis. Among each of the samples, the spectra bands of 0.25Ce-Fe/ZSM-5 sample increased faster than other samples and reached adsorption saturation earlier. This

result indicates that 0.25Ce-Fe/ZSM-5 sample possessed stronger acidity high acidity and strong NH₃ adsorption ability which was responsible for excellent NH₃-SCR performance.

4 CONCLUSION

After doping of Ce species, *x*Ce-Fe/ZSM-5 samples achieved better catalytic activity, large surface areas, high acidity and outstanding adsorption ability of NH₃. The efficiency of *x*Ce-Fe/ZSM-5 (*x*=0.25, 0.5 wt%) samples exhibited a NO conversion over 98% in 350-450 °C. XRD and BET experiments indicated that the Ce and Fe species are dispersed on the surface of the ZSM-5 zeolite with amorphous oxides and the crystal structure was maintained. Ce species significantly influenced the NH₃-SCR activity of the *x*Ce-Fe/ZSM-5 samples. XPS analysis suggested that the doping of Ce could generate more oxygen vacancies to increased the number of chemisorption oxygen. H₂-TPR analysis indicated that the doping of Ce created more isolated Ce⁴⁺ and Fe³⁺ on the surface of catalysts, and the abundant Ce⁴⁺ and Fe³⁺ could enhance the reduction ability of catalysts. The strength of acidity is a crucial factor in the NH₃-SCR reaction, and the NH₃-TPD results illustrated that the 0.25Ce-Fe/ZSM-5 sample possessed abundant medium and strong acid sites that are favorable to the adsorption and activity of NH₃, which is beneficial to the NH₃-SCR reaction.

Above all, 0.25Ce-Fe/ZSM-5 sample possessed abundant medium and strong Brønsted acid sites and remarkable adsorption ability of NH₃, outstanding redox ability and abundant chemisorption oxygen, exhibited excellent NH₃-SCR performance.

REFERENCES

1. J. A. Camargo and Á. Alonso, ENVIRON INT **32**, 6, 831 (2006).
2. Y. Shu, H. Wang, J. Zhu, and F. Zhang, CHEM RES CHINESE U **30**, 6, 1005 (2014).
3. A. Boubnov, H. W. P. Carvalho, D. E. Doronkin et al, J AM CHEM SOC **136**, 37, 13006 (2014).
4. M. Iwasaki, K. Yamazaki, K. Banno, and H. Shinjoh, J CATAL **260**, 2, 205 (2008).
5. C. K. Zheng, S. Han, X. Y. Liu, Q. Ye et al, Environmental Pollution Control **41**, 05, 520 (2019).
6. B. Liu, K. Zheng, Z. Liao, P. et al, IND ENG CHEM RES **59**, 18, 8592 (2020).
7. G. Qi and R. T. Yang, Applied Catalysis B: Environmental **60**, 1-2, 13 (2005).
8. M. Schwidder, M. Kumar, K. Klementiev et al, CATAL **231**, 2, 314 (2005).
9. S. Jiang and R. Zhou, FUEL PROCESS TECHNOL **133**, 220 (2015).
10. S. H. Begum, C. Hung, Y. Chen, S. Huang, P. Wu, X. Han, and S. Liu, Journal of Molecular Catalysis A: Chemical **423**, (2016).
11. M. Devadas, O. Kröcher, M. Elsener et al, CATAL TODAY **119**, 1-4, 137 (2007)
12. X. Yang, H. Xiao, J. Liu, Z. Wan, T. Wang, and B. Sun, Reaction kinetics, mechanisms and catalysis **125**, 2, 1071 (2018).
13. Z. Chen, L. Liu, H. Qu, Q. Zhong, and Z. Liu, CATAL LETT **150**, 2, 514 (2020).
14. S. Brandenberger, O. Kröcher, A. Wokaun, A. Tissler, and R. Althoff, J CATAL **268**, 2, 297 (2009).
15. M. Stanciulescu, P. Bulsink, G. Caravaggio et al, APPL SURF SCI **300**, 201 (2014).
16. L. Chen, X. Wang, Q. Cong, H. Ma, S. Li, and W. Li, CHEM ENG J **369**, 957 (2019).
17. X. Shi, Y. Wang, Y. Shan, Y. Yu, and H. He, J ENVIRON SCI-CHINA **94**, 32 (2020).